Biosensors and Bioelectronics 102 (2018) 87–93

Contents lists available at ScienceDirect

Biosensors and Bioelectronics

journal homepage: www.elsevier.com/locate/bios

A reusable ratiometric electrochemical biosensor on the basis of the binding of methylene blue to DNA with alternating AT base sequence for sensitive detection of adenosine

Lin Cui[a,1], Mengfei Lu[a,1], Ying Li[b,1], Bo Tang[a], Chun-yang Zhang[a,*]

[a] College of Chemistry, Chemical Engineering and Materials Science, Collaborative Innovation Center of Functionalized Probes for Chemical Imaging in Universities of Shandong, Key Laboratory of Molecular and Nano Probes, Ministry of Education, Shandong Provincial Key Laboratory of Clean Production of Fine Chemicals, Shandong Normal University, Jinan 250014, PR China

[b] School of Medicine, Health Science Center,Shenzhen University, Shenzhen 518060, PR China

ARTICLE INFO

Keywords:
Electrochemical biosensor
Ratiometric analysis
Aptamer
Adenosine
Sensitivity
Regeneration capability

ABSTRACT

We develop a reusable ratiometric electrochemical biosensor on the basis of the binding of methylene blue (MB) to DNA with alternating AT base sequence for sensitive detection of adenosine. We design a strand 1 with MB-modified thymine (T) base in the proximal 3′ termini as the capture probe for its immobilization on the gold electrode and a 3′ termini ferrocene (Fc)-modified aptamer for the recognition of adenosine. The hybridization of strand 1 with the aptamer leads to the formation of a double-stranded DNA (dsDNA) and consequently the away of MB from the electrode surface and the close of Fc to the electrode surface, generating a small value of I_{MB}/I_{Fc} (I_{MB} and I_{Fc} are the peak currents of MB and Fc, respectively). In the presence of adenosine, its binding with the aptamer induces the release of Fc from the electrode surface and the close of MB to the electrode surface, generating a large value of I_{MB}/I_{Fc}. As a result, adenosine may be accurately quantified by the measurement of ratiometric signal (I_{MB}/I_{Fc}). This ratiometric electrochemical biosensor can be simply fabricated and exhibits high sensitivity with a limit of detection of as low as 90.8 pM and a large dynamic range from 0.1 nM to 100 μM. Moreover, this biosensor demonstrates good performance with excellent selectivity, regeneration capability, high reliability and good reproducibility, and may become a universal platform for the detection of various biomolecules which can be recognized by aptamers, holding great potential for further applications in biomedical research and clinical diagnosis.

1. Introduction

Electrochemical biosensors have distinct characteristics of easy fabrication, simple signal generation, and convenient miniaturization and integration, and have been widely applied in the design of portable detection devices (Rowe et al., 2011; Wu et al., 2011; Wu and Lai, 2016; Xiao et al., 2009, 2007a; Yang and Zhang, 2010). A number of electrochemical DNA (E-DNA) sensors have been developed on the basis of that the hybridization-induced conformational changes may significantly alter the electron transfer from a redox-tagged electrode-bound DNA probe to the electrode (Abi and Ferapontova, 2012; Dauphin-Ducharme and Plaxco, 2016; Du et al., 2014; Wu and Lai, 2013; Xiao et al., 2007a). Plaxco group demonstrated the development of a series of E-DNA sensors based on the binding-induced conformational changes for the detection of proteins (Lai et al., 2007; Xiao et al., 2005a, 2005b), heavy metal ions (Xiao et al., 2007b) and DNAs (Fan et al., 2003; Xiao et al., 2006, 2007a). A barrier to the wide adoption of these electrochemical biosensors is the issues related to the reproducibility, robustness and reliability, which result from the hard-to-avoid variations in electrode areas, DNA loading densities, and nontarget-induced reagent degradation/dissociation. The idiosyncratic background currents observed in disparate electrodes make it difficult to accurately detect target analyst in spite of the involvement of time-consuming background scans for each new electrode and each new analysis. Therefore, the development of a reusable ratiometric electrochemical biosensor with good reproducibility, robustness and reliability is highly desirable.

The ratiometric measurement has been extensively employed in various analytical techniques such as fluorescence (Dai et al., 2015; Liu et al., 2014), electrochemistry (Chai et al., 2014; Cheng et al., 2015; Jin

* Corresponding author.
E-mail addresses: tangb@sdnu.edu.cn (B. Tang), cyzhang@sdnu.edu.cn (C.-y. Zhang).
[1] These authors contributed equally.

http://dx.doi.org/10.1016/j.bios.2017.11.025
Received 6 October 2017; Received in revised form 2 November 2017; Accepted 5 November 2017
Available online 07 November 2017
0956-5663/

et al., 2017; Ren et al., 2015; Wang et al., 2017; Zhang et al., 2015), electrochemiluminescence (Feng et al., 2015; Zhang et al., 2013) and photoelectrochemistry (Hao et al., 2016). Among them, the ratiometric electrochemical biosensor has attracted increasing attention because of its rapid response, simplicity and cost-effectiveness. The ratiometric measurement has the capability of self-reference by removing the signal fluctuation caused by complex experimental conditions (Cui et al., 2017), and greatly improves the reproducibility and robustness of electrochemical biosensors. The ferrocene (Fc) and methylene blue (MB) are usually used as the internal references for ratiometric measurement of proteins (Deng et al., 2016; Ren et al., 2014; Wang et al., 2017), DNAs (Cui et al., 2017; Du et al., 2014; Xiong et al., 2015), and other analysts (Jia et al., 2016; Xiong et al., 2015). In comparison with the single-signal readout, the ratio calculation of dual-signal readouts may significantly improve the detection sensitivity (Wu et al., 2013). So far, most of the reported ratiometric electrochemical biosensors are developed on the basis of the binding-induced conformational changes of terminal redox-tagged DNA, and the electrochemical response induced by only DNA-mediated electron transfer relies on the tuning of the probe structural flexibility with the limitations of high background and poor sensitivity (Campos et al., 2014; Rowe et al., 2011; Xiao et al., 2009; Yang et al., 2014). Notably, the electron transfer between the redox tag and the electrode is also dependent on the way of the redox tag conjugated to the DNA duplex (e.g., intercalation and groove binding) (Hsieh et al., 2011; Lubin et al., 2009; Rohs et al., 2000; Tuite et al., 1994; Wang et al., 2015). Rohs et al. investigated the binding behavior of methylene blue (MB) to a double-stranded decamer, with a groove binding mode for DNA with AT sequences (Rohs et al., 2000) and an intercalation binding mode for GC alternating DNA (Rohs et al., 2004). Hsieh et al. developed an electrochemical biosensor for the identification of single-nucleotide mismatches based on the principle that the interaction between MB and poly(thymine–adenosine) (T-A) duplexes may effectively slow down MB electron transfer rate (Hsieh et al., 2011). To the best of our knowledge, a reusable ratiometric electrochemical biosensor on the basis of the binding of methylene blue to DNA with alternating AT base sequence has never been reported so far.

Herein, we demonstrate the development of a reusable ratiometric electrochemical biosensor on the basis of the binding of methylene blue to DNA with alternating AT base sequence for sensitive detection of adenosine. We design a strand 1 with MB-modified thymine (T) base in the proximal 3′ termini as the capture probe for its immobilization on the gold (Au) electrode and a 3′ termini ferrocene (Fc)-modified aptamer for the recognition of adenosine (the aptamer binds adenosine with a dissociation constant (K_d) of 6 μM (Huizenga and Szostak, 1995)). In the presence of adenosine, its binding with the aptamer induces the release of Fc from the electrode surface and the close of MB to the electrode surface, generating a large value of I_{MB}/I_{Fc} (I_{MB} and I_{Fc} are the peak currents of MB and Fc, respectively). The measurement of ratiometric signal (I_{MB}/I_{Fc}) can be used for accurate quantification of adenosine. This ratiometric biosensor exhibits high sensitivity with a limit of detection of as low as 90.8 p.M. and a large dynamic range from 0.1 nM to 100 μM, and it performs well in real sample analysis with distinct advantages of excellent selectivity, regeneration capability, high reliability and good reproducibility.

2. Materials and methods

2.1. Materials and reagents

Mercaptohexanol (MCH), tris-(2-carboxyethyl) phosphine hydrochloride (TCEP), tris-(hydroxymethyl)aminomethane (Tris), adenosine, adenosine monophosphate (AMP), adenosine diphosphate (ADP), adenosine triphosphate (ATP), cytidine, guanosine and uridine were obtained from Sigma-Aldrich Chemical Co. (St. Louis, MO, USA). All solutions were prepared with ultrapure water obtained from a Milli-Q water purification system (Millipore, Milford, MA, USA) with a resistivity of 18.2 MΩ cm. All of the oligonucleotides were synthesized and purified with HPLC by Takara Biotech. Co. Ltd. (Dalian, China) and their sequences were listed in Table S1.

2.2. Fabrication of electrochemical biosensor

Prior to the modification, the Au electrode was polished to a mirror-like surface with 1.0, 0.3 and 0.05 μm α-Al_2O_3 slurry, respectively, followed by successive sonication with ethanol and ultrapure water for 3 min to remove residual alumina powder. The electrode was immersed into fresh piranha solution (3:1 v/v mixture of concentrated H_2SO_4 and 30% H_2O_2) for 10 min, followed by a thorough rinse with ultrapure water and drying by nitrogen. Then the electrode was electrochemically cleaned in 0.1 M H_2SO_4 solution by potential scanning between −0.2 and +1.6 V at a scan rate of 100 mV s^{-1} until a stable reproducible cyclic voltammogram was obtained.

After washing with ultrapure water and drying in a nitrogen stream, the electrode was incubated with 6 μL of solution containing 0.5 μM strand 1 and 25 μM TCEP (TCEP is used to reduce the disulfide bonded oligonucleotides) at room temperature for 12 h to make strand 1 immobilize onto the gold electrode surface via gold-sulfur chemistry. The electrode was then thoroughly rinsed with 10 mM PBS (pH 7.4) and dried under a stream of nitrogen gas. Subsequently, 6 μL of 1 mM MCH was dropped on the electrode for 60 min to block the unmodified sites. After rinsing thoroughly with 10 mM PBS (pH 7.4), the electrode was incubated with aptamer conjugates in 10 mM PBS (pH 7.4) containing 100 mM NaCl at 37 °C for 2 h. At last, the electrode was thoroughly rinsed and stored at 4 °C prior to use.

2.3. Detection of adenosine and regeneration of electrochemical biosensor

The 10 μL of adenosine with different concentrations was added into the electrochemical biosensor and incubated at 37 °C for 1 h. Then the electrode was thoroughly washed three times with PBS buffer. For the measurement of adenosine, alternating-current voltammetry (ACV) responses of the ratiometric probes before and after the addition of adenosine were monitored in10 mM PBS (pH 7.4) (note: 10 mM PBS (pH 7.4) should be completely purged with high purity nitrogen for 30 min to avoid the interference from the reduction of oxygen prior to the measurement). Finally, the aptamers were added onto the modified electrode to regenerate the electrochemical biosensor.

2.4. Electrochemical measurement

All electrochemical measurements were carried out on a CHI 660e electrochemical workstation (CH Instruments Inc., USA) at room temperature with a conventional three-electrode system composed of a platinum wire, a saturated calomel and a gold electrode (d = 2 mm) as the counter, reference and working electrodes, respectively. Cyclic voltammetry (CV) measurements were carried out in scanning potential from −0.2 to 0.6 V with 5 mM $[Fe(CN)_6]^{3-/4-}$ (containing 0.1 M KCl) as the electrolyte. Electrochemical impedance spectroscopic (EIS) measurements were performed in 5 mM $[Fe(CN)_6]^{3-/4-}$ redox couple solution (1:1 M ratio) containing 0.1 M KCl over a frequency range from 10 kHz to 0.1 Hz using an alternative voltage with an amplitude of 10 mV, superimposed on a dc potential of 0.20 V (vs SCE). The ACV was performed using a potential window of −0.5 to +0.6 V with a pulse amplitude of 50 mV and a pulse width of 200 ms in 5 mL of 10 mM PBS (pH 7.4) buffer. The chronocoulometry measurements were carried out over a range from +0.2 to −0.5 V at a pulse period of 250 ms in 10 mM Tris-HCl buffer containing 50 μM $Ru(NH_3)_6^{3+}$ (pH 7.4).

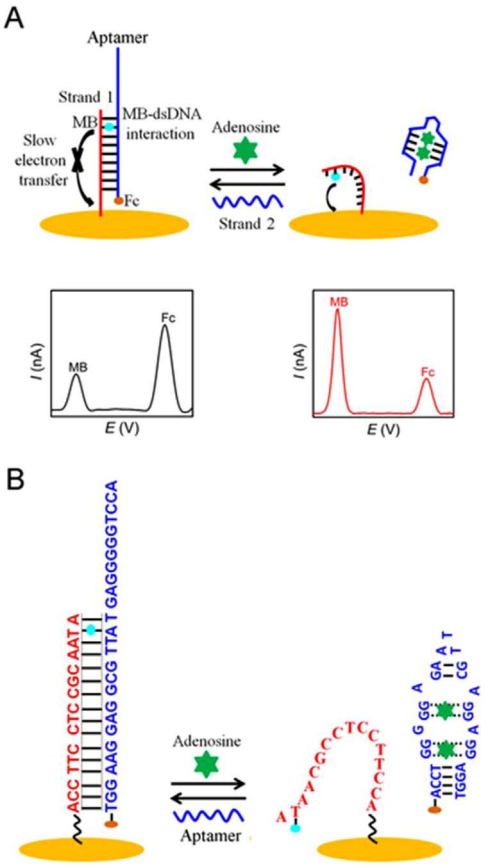

Scheme 1. (A) The principle of ratiometric electrochemical biosensor for the detection of adenosine. (B) The design of a thiolated strand 1 modified with MB at thymine (T) base of its proximal 3′ terminus as the capture probe for its immobilization onto the Au electrode surface and a 3′ termini Fc-modified aptamer for the recognition of adenosine. The hybridization of strand 1 with the aptamer leads to the formation of dsDNA and consequently the away of MB from the electrode surface and the close of Fc to the electrode surface, generating a small value of I_{MB}/I_{Fc} (I_{MB} and I_{Fc} are the peak currents of MB and Fc, respectively). In the presence of adenosine, its binding with the aptamer induces the release of Fc from the electrode surface and the close of MB to the electrode surface, generating a large value of I_{MB}/I_{Fc}.

3. Results and discussion

3.1. Principle of ratiometric electrochemical biosensor

The principle of ratiometric electrochemical biosensor is shown in Scheme 1. We designed a thiolated strand 1 modified with MB at thymine (T) base of its proximal 3′ terminus (Table S1) as the capture probe for its immobilization onto the Au electrode surface via Au-S covalent bond and a 3′ termini Fc-modified aptamer for the recognition of adenosine, with MB and Fc as the electroactive molecules for the generation of electrochemical signals. The hybridization of strand 1 with the aptamer leads to the formation of a rigid dsDNA and consequently the away of MB from the electrode surface and the close of Fc to the electrode surface, generating a small value of I_{MB}/I_{Fc} (I_{MB} and I_{Fc} are the peak currents of MB and Fc, respectively). Notably, the small I_{MB} value results from not only the relatively far away of MB from the electrode surface but also its interaction with poly(thymine–adenosine) (T-A) duplexes (Hsieh et al., 2011; Rohs and Sklenar, 2004; Tuite and Norden, 1994) which can retard the electron transfer. The high I_{Fc} value can be attributed to the confinement of Fc near the electrode surface as a result of the formation of dsDNA (Scheme 1). In this research, a short 6-mercapto-1-hexanol is used to passivate the electrochemical biosensor for the avoidance of nonspecific adsorption. While in the presence of adenosine, the Fc-modified aptamer can form a G-quadruplex with adenosine and subsequently dissociates from the dsDNA complex into solution, leaving a flexible strand 1 on the electrode surface (Zhang et al., 2017). Consequently, the binding of adenosine with the aptamer induces the release of Fc from the electrode surface and the close of MB to the electrode surface, generating a large value of I_{MB}/I_{Fc}. As a result, adenosine may be accurately quantified by the measurement of ratiometric signal (I_{MB}/I_{Fc}). Notably, the formation of aptamer-adenosine structure guarantees the good selectivity, and the groove binding of MB tag with the poly-T-A region of dsDNA ensures the low MB background current and high detection sensitivity. In addition, this ratometric electrochemical biosensor is readily reusable by reaction with the aptamer.

3.2. Characterization of electrochemical biosensor

We employed cyclic voltammograms and electrochemical impedance spectra to characterize the assembly processes of gold electrode with $[Fe(CN)_6]^{4-/3-}$ as the electroactive probe. In cyclic voltammetric measurements, the peak currents and the separation of peak potential (ΔE_p) changes are used to reflect the electron transfer of redox probe at the sensing interface. As shown in Fig. S1A, the bare gold electrode exhibits a larger redox peak current and a well-defined redox peak of $[Fe(CN)_6]^{3-/4-}$ with a ΔE_p of 95 mV (Fig. S1A**, curve a**), indicating the fast electron transfer of redox probe. The self-assembly of strand 1 onto the bare Au electrode induces the decrease of redox peak current and the increase of ΔE_p to 147 mV (Fig. S1A**, curve b**) due to the blocking of interfacial electron transfer by strand 1. The subsequent self-assembly of MCH onto the strand 1/Au electrode may block the remaining active sites, resulting in the decrease of redox peak current and the increase of ΔE_p (Fig. S1A**, curve c**). After further assembly of aptamer onto the MCH/strand 1/Au electrode surface, the negative charged DNA may prevent the diffusion of ferricyanide toward the electrode surface, leading to the decrease of redox peak current and the increase of peak-to-peak separation (Fig. S1A**, curve d**). In the presence of adenosine, aptamer dissociates from the dsDNA complex to form a G-quadruplex-adenosine complex, leaving a flexible strand 1 on the electrode surface and inducing the increase of peak current and the decrease of ΔE_p (Fig. S1A**, curve e**).

The electrochemical impedance spectra (EIS) were used for interfacial study. The electron-transfer resistance (R_{et}) is controlled by the electron transfer kinetics of $[Fe(CN)_6]^{3-/4-}$ on the modified Au electrodes, and it can be characterized by the semicircle diameter of Nyquist plot. As shown in Fig. S1B, the bare Au electrode displays a small semicircle diameter and a long tail, indicating the diffusion of $[Fe(CN)_6]^{3-/4-}$ (Fig. S1B**, curve a**). In contrast, the strand 1-modified Au electrode exhibits a higher R_{et} (Fig. S1B**, curve b**), because the immobilization of negatively charged strand 1 onto the electrode surface may result in a negatively charged interface that electrostatically repels the negatively charged redox probe $[Fe(CN)_6]^{3-/4-}$ and inhibits the interfacial charge transfer. The subsequent surface blocking by MCH can induce the increase of R_{et} (Fig. S1B**, curve c**), because the short alkanethiol provides an insufficient barrier to block the electron transfer. After assembly of aptamer onto the MCH/strand 1/Au electrode surface, the electrode interface becomes more negatively charged due to the absorption of negatively charged DNA, leading to a further increase of R_{et} (Fig. S1B**, curve d**). On the contrary, the presence of adenosine causes significant decrease of R_{et} (Fig. S1B**, curve e**) due to the release of aptamers from the gold electrode surface induced by the formation of adenosine-aptamer complexes. These results clearly demonstrate the success fabrication of electrochemical sensing interface for adenosine assay.

3.3. Assay feasibility

We used three different MB modification strategies to optimize the MB background current (Fig. 1A-C): one with MB modified on the

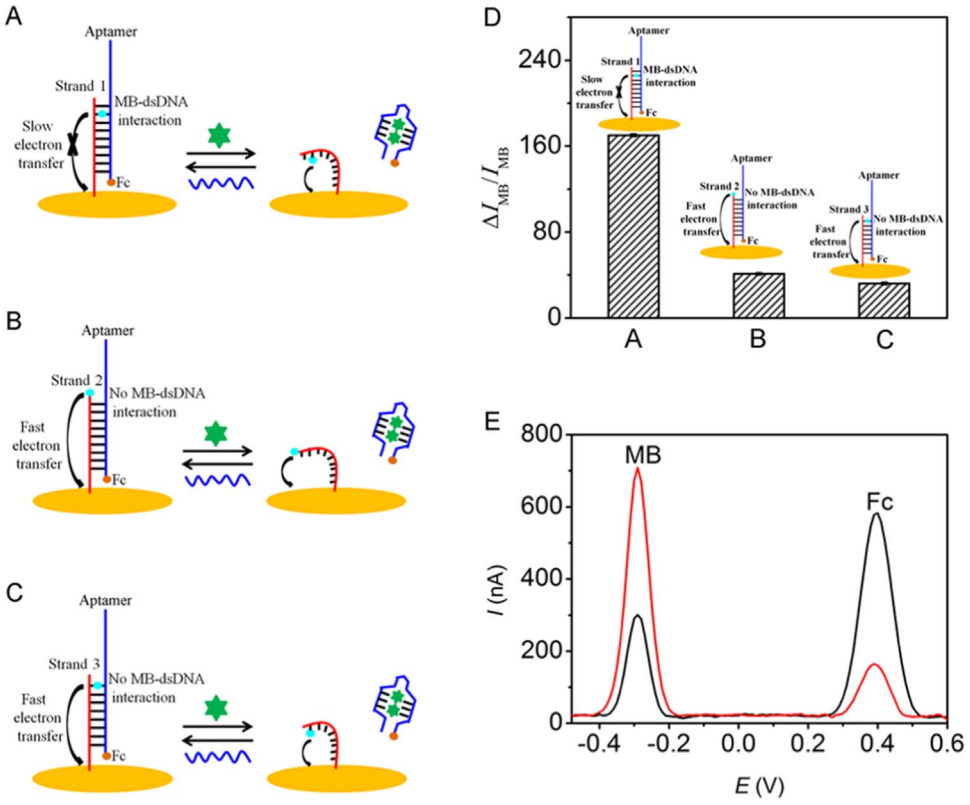

Fig. 1. Comparison of ratiometric electrochemical biosensor with MB modified on the second base of 3′ terminal (A), the hydroxyl of the 3′ terminal (B), and the thymidine of the 3′ terminal (C). (D) Comparison of the increasing ratio of MB peak current induced by MB modification on the second base of 3′ terminal (column A), the hydroxyl of the 3′ terminal (column B), and the thymidine of the 3′ terminal (column C). (E) ACV responses of ratiometric electrochemical biosensor in the absence (black curve) and presence (red curve) of 100 nM adenosine. The error bars represent the standard deviation of three independent experiments.

thymidine that is the second base from the 3′ terminal of strand 1 (Fig. 1A) and two controls with MB being modified on the hydroxyl of the 3′ terminal (strand 2) (Fig. 1B) and on the thymidine of the 3′ terminal (strand 3) (Fig. 1C). To evaluate the performance of three different modification strategies, we used $\frac{\Delta I_{MB}}{I_{MB}} = \frac{I'_{MB} - I_{MB}}{I_{MB}}$ to describe the increasing ratio of MB peak current, in which $I_{MB}$is the ACV peak current in the absence of adenosine and I'_{MB} is the ACV peak current in the presence of 100 nM adenosine. As shown in Fig. 1D, the biosensor with MB modified on the second base of 3′ terminal induces the increase of MB redox peak current by as much as 170.3% ± 8.8% (Fig. 1D (A)), much higher than those biosensors with MB modified on the hydroxyl of the 3′ terminal (41.6% ± 4.5%) (Fig. 1D (B)) and on the thymidine of the 3′ terminal (32.2% ± 6.3%) (Fig. 1D (C)), suggesting that the interaction of MB with the poly(thymine–adenine)duplex may effectively slow down the MB electron transfer rate (Hsieh et al., 2011; Rohs and Sklenar, 2004). This result (Fig. 1D) clearly demonstrates that the change in the output Faradaic current is caused by the alterations in the rate of electron transfer to the gold interrogating electrode, which is governed by the equilibrium probability of the DNA-bound MB tag approaching the electrode surface.

The feasibility of ratiometric electrochemical biosensor is further confirmed by the measurement of ACV. As is shown in Fig. 1E, a low oxidation peak of MB at −0.28 V and a high oxidation peak of Fc at +0.39 V are observed in the absence of adenosine (**black curve**), indicating the successful construction of dsDNA-modified Au electrode with two well-distinguished potentials corresponding to two electroactive molecules (Fc and MB), respectively. In the presence of 100 nM adenosine, the MB electrochemical signal significantly increases, accompanied by the decrease of Fc electrochemical signal (**red curve**), because the formation of aptamer-adenosine complexes induces the dissociation of aptamers from the electrode surface and consequently the away of Fc from the electrode surface and the close of MB to the electrode surface. These results further demonstrate the feasibility of the ratiometric electrochemical biosensor for adenosine assay.

3.4. Optimization of experimental conditions

To achieve the best performance of ratiometric electrochemical biosensor, we optimized the experimental parameters including the immobilization concentration of strand 1 and the reaction time (Fig. S2). We first investigated the effect of the immobilization concentration of strand 1 on the ratiometric electrochemical response (I_{MB}/I_{Fc}) of the biosensor in the presence of 100 nM adenosine. Fig. S2A shows the variance of I_{MB}/I_{Fc} value with the concentration of strand 1. The I_{MB}/I_{Fc} value enhances with the increasing concentration of strand 1 from 0.05 to 1 μM, followed by decrease beyond the concentration of 0.5 μM due to the increased steric hindrance at high immobilization concentration of strand 1 which can prevent the target binding-induced aptamer conformational change. Thus, 0.5 μM strand 1 is used in the subsequent experiments. We investigated the influence of reaction time upon the I_{MB}/I_{Fc} value as well. As shown in Fig. S2B, the I_{MB}/I_{Fc} value increases with the reaction time from 10 to 120 min, and levels off at 70 min. Thus, the reaction time of 70 min is used in the subsequent experiments.

3.5. Quantitation of DNA density on the electrode surface

The amount of strand 1 immobilized on the electrode surface may be determined through the measurement of the adsorbed $[Ru(NH_3)_6]^{3+}$ by using chronocoulometry on the basis of integrated Cottrell equation (Steel et al., 1998):

$$Q = \frac{2nFAD_0^{1/2}C_0^*}{\pi^{1/2}}t^{1/2} + Q_{dl} + nFA\Gamma_0 \quad (1)$$

Where Q represents the charge owing to the reaction of $[Ru(NH_3)_6]^{3+}$that diffuses to the electrode surface, Q_{dl} is the capacitive charge, and $nFA\Gamma_0$ represents the charge produced by the adsorbed $[Ru(NH_3)_6]^{3+}$. The amount of $[Ru(NH_3)_6]^{3+}$ adsorbed to the phosphate backbone of the immobilized DNA (Γ_0), which can be determined from the difference in intercepts (Δ_{int}) at $t = 0$ in the presence and absence of

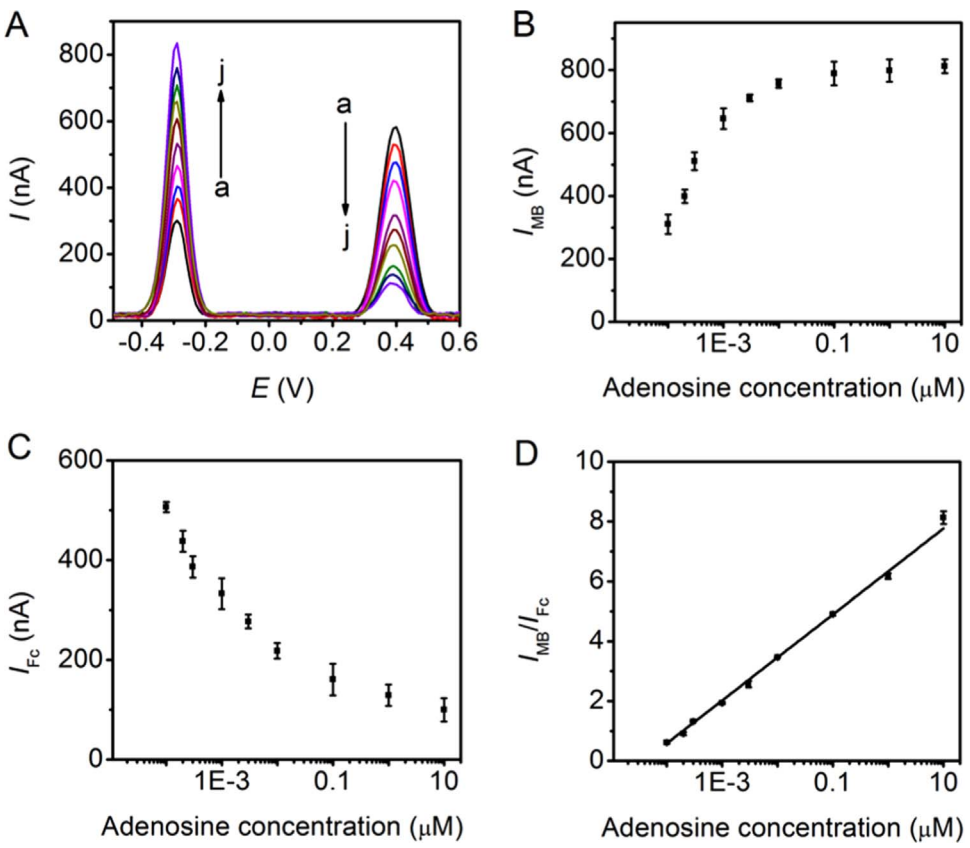

Fig. 2. (A) Variance of ACV peak current in response to different-concentration adenosine: (a) 0, (b) 0.1 nM, (c) 0.2 nM, (d) 0.3 nM, (e) 1 nM, (f) 3 nM, (g) 10 nM, (h) 100 nM, (i) 1 μM and (j) 10 μM. (B) Logarithmic dependence of MB electrochemical signal upon the concentration of adenosine. (C) Logarithmic dependence of Fc electrochemical signal upon the concentration of adenosine. (D) Logarithmic dependence of the ACV peak current ratio of I_{MB}/I_{Fc} upon the concentration of adenosine. The error bars represent the standard deviation of three independent experiments.

$[Ru(NH_3)_6]^{3+}$, is quantitative to the quantity of the immobilized DNA (Γ_{DNA}) by dividing the number of bases in the single immobilized DNA strand (Zhang et al., 2006):

$$\Gamma_{DNA} = \Gamma_0(z/m)(N_A) \quad (2)$$

Where Γ_{DNA} is the strand 1 surface density, m is the number of bases in the strand 1, z is the charge of redox molecule, and N_A is Avogadro's number. Based on the chronocoulometric responses of $[Ru(NH_3)_6]^{3+}$ (Fig. S3), the surface density of strand 1 on the gold electrode surface is estimated to be 2.67×10^{12} molecules cm^{-2}.

3.6. Sensitivity of ratiometric electrochemical biosensor

Under the optimally experimental conditions, the sensitivity of ratiometric electrochemical biosensor was evaluated by monitoring the ACV peak current ratio (I_{MB}/I_{Fc}) in response to different-concentration adenosine. As shown in Fig. 2A, the ACV peak current ratio of I_{MB}/I_{Fc} improves with the increasing concentration of adenosine. In logarithmic scale, the I_{MB}/I_{Fc} value exhibits a linear correlation with the adenosine concentration over a range of 5 orders of magnitude from 0.1 nM to 10 μM (Fig. 2D). The regression equation is $I_{MB}/I_{Fc} = 1.437 \log_{10}C + 6.332$ with a correlation coefficient of 0.998. The limit of detection (LOD) is calculated to be 90.8 pM by evaluating the blank plus 3 standard deviations of the blank. The sensitivity of this ratiometric electrochemical biosensor has improved by at least 2 orders of magnitude as compared with those of fluorescent assay (Ahn et al., 2017; Fu et al., 2013; Huang et al., 2016; Huang and Liu, 2010; Liao et al., 2012; Song et al., 2012; Sun et al., 2015) and surface-enhanced Raman scattering assay (Chen et al., 2008), 2–55-fold as compared with that of electrochemical assay (Sun et al., 2010; Zhang et al., 2008), and is comparable to that of photoelectrochemical assay (Liu et al., 2016) (Table S2). In addition, the LOD obtained by the biosensor with individual electrochemical indicator is 3.3 nM for MB (Fig. 2B) and 4.6 nM for Fc (Fig. 2C), much poorer than that obtained by the ratiometric electrochemical biosensor (90.8 pM). These results clearly demonstrate the high sensitivity of ratiometric electrochemical biosensor for adenosine assay. It is worth noting that the ratiometric electrochemical biosensor exhibits a wider dynamic range and a lower LOD than the electrochemical biosensors with either MB modified on the 3′ end (1 nM ~ 10 μM, 0.31 nM) (Fig. 3A) or MB modified on the T base of the 3′ end (1 nM ~ 10 μM, 0.56 nM) (Fig. 3B)

3.7. Selectivity, stability and reproducibility of ratiometric electrochemical biosensor

To evaluate the selectivity of ratiometric electrochemical biosensor, we used ATP, ADP, AMP, guanosine, cytidine and uridine as the nonspecific interferences. These nonspecific interferences are analogous molecules of adenosine but have different molecular structure. We monitored the ACV peak current ratio of I_{MB}/I_{Fc} in response to adenosine, the nonspecific interferences and the mixture, respectively. As shown in Fig. 4, a high I_{MB}/I_{Fc} value is obtained in the presence of 100 nM adenosine and the mixture containing nonspecific interferences (each at 1 μM) and adenosine (100 nM), but no significant I_{MB}/I_{Fc} value is observed even in the presence of 1 μM nonspecific interferences. Notably, the mixture of nonspecific interferences (each at 1 μM) and adenosine (100 nM) generate same level of I_{MB}/I_{Fc} value as 100 nM adenosine alone, suggesting that this ratiometric electrochemical biosensor is highly selective towards adenosine. Such high selectivity may be ascribed to the specific binding of aptamer with adenosine and the subsequent target binding-induced aptamer conformational changes (Shen et al., 2017; Feng et al., 2016; Zhu et al., 2011).

We further investigated the stability and reproducibility of ratiometric electrochemical biosensor by repetitively monitoring 100 nM adenosine. The relative standard deviation (R.S.D.) of peak currents was calculated to be 4.5% ($n = 6$), and no significant change in peak current was observed even after two-week storage at 4 °C, suggesting the excellent stability of ratiometric electrochemical biosensor. The

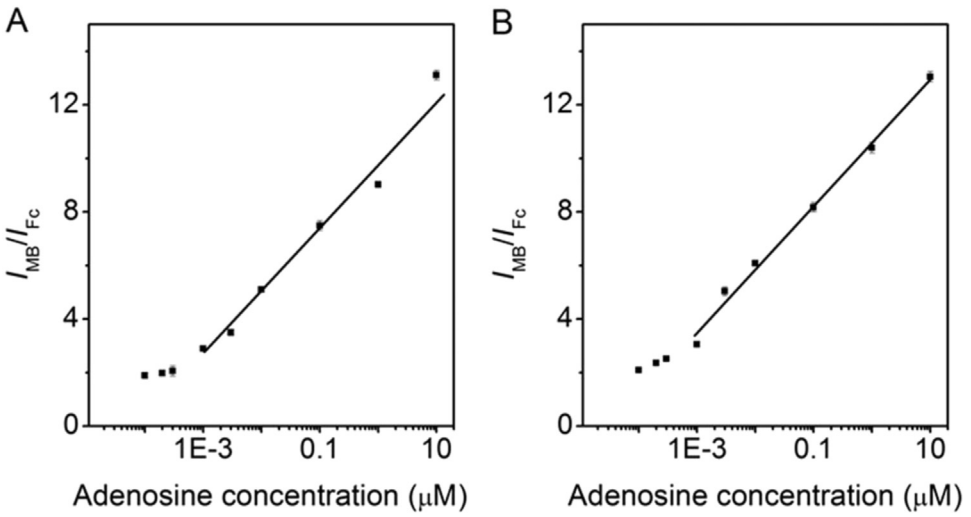

Fig. 3. Logarithmic dependence of the ACV peak current ratio of I_{MB}/I_{Fc} upon the concentration of adenosine with MB modified on the 3′ end (A) and MB modified on the T base of the 3′ end (B). The error bars represent the standard deviation of three independent experiments.

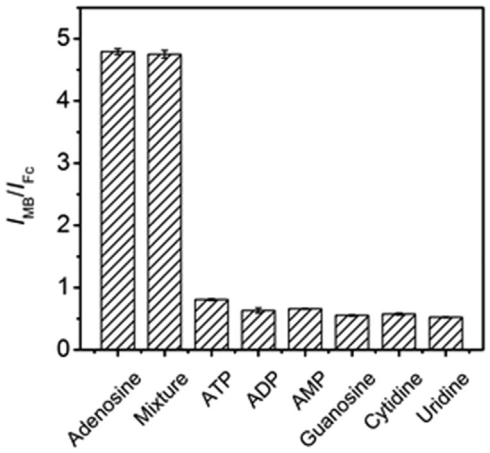

Fig. 4. Selectivity of ratiometric electrochemical biosensor towards adenosine. Adenosine (100 nM), ATP (1 μM), ADP (1 μM), AMP (1 μM), guanosine (1 μM), cytidine (1 μM) and uridine (1 μM) were used in this research. The reaction time is 70 min, and the reaction temperature is 37 °C. Error bars represent the standard deviation of three independent experiments.

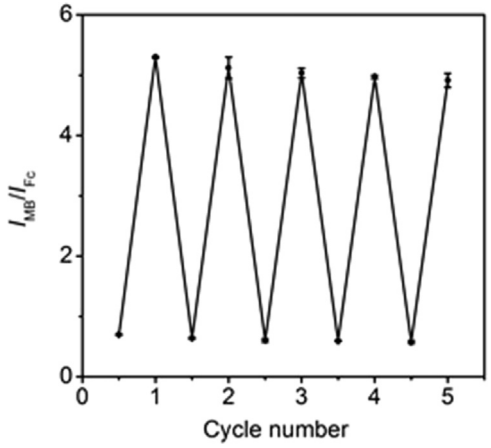

Fig. 5. Regeneration of ratiometric electrochemical biosensor under the stepwise hybridization with adenosine and then with aptamer over 5 cycles.

reproducibility was investigated by preparing six electrodes from same batch for the detection of same-concentration adenosine. The obtained R.S.D. was 5.1%, indicating good reproducibility of ratiometric electrochemical biosensor.

3.8. Regeneration of ratiometric electrochemical biosensor

Another important parameter of ratiometric electrochemical biosensor is its reusability in practical applications. This ratiometric electrochemical biosensor may be easily regenerated by incubation in 0.5 μM aptamer at 37 ℃ for 60 min to form the hybridized duplex. Even after repeating this regeneration process for 5 cycles, this electrochemical biosensor still retains its original hybridization efficiency with a standard deviation of 4.8% (Fig. 5). This result clearly demonstrates the good regenerability of ratiometric electrochemical biosensor.

3.9. Serum sample analysis

To demonstrate the feasibility of ratiometric electrochemical biosensor for real sample analysis, we measured the recoveries of different-concentration adenosine in 1:10 diluted human serum samples. As shown in Table S3, the recoveries of adenosine spiked in human serum sample were 97.6% for 0.001 μM adenosine, 94.6% for 0.01 μM adenosine, 115% for 0.1 μM adenosine, and 97.8% for 1 μM adenosine, with the relative standard deviation of 3.1%, 1.4%, 4.7% and 3.1%, respectively, suggesting the good accuracy of ratiometric electrochemical biosensor for real sample analysis.

4. Conclusions

In summary, we have developed a reusable ratiometric electrochemical biosensor for adenosine assay on the basis of the binding of methylene blue (MB) to DNA with alternating AT base sequence. The sensitivity of this ratiometric biosensor may be greatly improved by embedding methylene blue to the DNA groove, and the background signal may be efficiently eliminated by the introduction of ratiometric measurement. This ratiometric biosensor can be simply fabricated and exhibits high sensitivity with a limit of detection of as low as 90.8 pM and a large dynamic range from 0.1 nM to 100 μM, superior to the reported biosensors for adenosine assay (Table S2). Moreover, this ratiometric biosensor demonstrates good performance with excellent selectivity, regeneration capability, high reliability and good reproducibility, and may become a universal platform for the detection of various biomolecules which can be recognized by aptamers, holding great potential for further applications in biomedical research and clinical diagnosis.

Acknowledgments

This work was supported by the National Natural Science Foundation of China (Grant Nos. 21325523 and 21527811, 21735003, 21605096 and 31400655), and the Award for Team Leader Program of Taishan Scholars of Shandong Province, China.

Appendix A. Supporting information

Supplementary data associated with this article can be found in the online version at http://dx.doi.org/10.1016/j.bios.2017.11.025.

References

Abi, A., Ferapontova, E.E., 2012. J. Am. Chem. Soc. 134, 14499–14507.
Ahn, J.K., Kim, H.Y., Baek, S., Park, H.G., 2017. Biosens. Bioelectron. 93, 330–334.
Campos, R., Kotlyar, A., Ferapontova, E.E., 2014. Langmuir 30, 11853–11857.
Chai, X., Zhang, L., Tian, Y., 2014. Anal. Chem. 86, 10668–10673.
Chen, J.-W., Liu, X.-P., Feng, K.-J., Liang, Y., Jiang, J.-H., Shen, G.-L., Yu, R.-Q., 2008. Biosens. Bioelectron. 24, 66–71.
Cheng, H., Wang, X., Wei, H., 2015. Anal. Chem. 87, 8889–8895.
Cui, L., Lu, M., Yang, X.-Y., Tang, B., Zhang, C.-Y., 2017. Analyst 142, 1562–1568.
Dai, C., Yang, C.-X., Yan, X.-P., 2015. Anal. Chem. 87, 11455–11459.
Dauphin-Ducharme, P., Plaxco, K.W., 2016. Anal. Chem. 88, 11654–11662.
Deng, C., Pi, X., Qian, P., Chen, X., Wu, W., Xiang, J., 2016. Anal. Chem. 89, 966–973.
Du, Y., Lim, B.J., Li, B., Jiang, Y.S., Sessler, J.L., Ellington, A.D., 2014. Anal. Chem. 86, 8010–8016.
Fan, C., Plaxco, K.W., Heeger, A.J., 2003. Proc. Natl. Acad. Sci. USA 100, 9134–9137.
Feng, C.J., Hou, Z., Jiang, W., Sang, L.H., Wang, L., 2016. Biosens. Bioelectron. 86, 966–970.
Feng, Q.-M., Shen, Y.-Z., Li, M.-X., Zhang, Z.-L., Zhao, W., Xu, J.-J., Chen, H.-Y., 2015. Anal. Chem. 88, 937–944.
Fu, B., Cao, J., Jiang, W., Wang, L., 2013. Biosens. Bioelectron. 44, 52–56.
Hao, Q., Shan, X., Lei, J., Zang, Y., Yang, Q., Ju, H., 2016. Chem. Sci. 7, 774–780.
Hsieh, K., White, R.J., Ferguson, B.S., Plaxco, K.W., Xiao, Y., Soh, H.T., 2011. Angew. Chem. Int. Ed. 50, 11176–11180.
Huang, H., Yang, X., Wang, K., Wang, Q., Guo, Q., Huang, J., Liu, J., Song, C., 2016. Analyst 141, 2502–2507.
Huang, P.-J.J., Liu, J., 2010. Anal. Chem. 82, 4020–4026.
Huizenga, D.E., Szostak, J.W., 1995. Biochemistry 34, 656–665.
Jia, J., Chen, H.G., Feng, J., Lei, J.L., Luo, H.Q., Li, N.B., 2016. Anal. Chim. Acta 908, 95–101.
Jin, H., Gui, R., Yu, J., Lv, W., Wang, Z., 2017. Biosens. Bioelectron. 91, 523–537.
Lai, R.Y., Plaxco, K.W., Heeger, A.J., 2007. Anal. Chem. 79, 229–233.
Liao, D., Jiao, H., Wang, B., Lin, Q., Yu, C., 2012. Analyst 137, 978–982.
Liu, L., Yang, Q., Lei, J., Xu, N., Ju, H., 2014. Chem. Commun. 50, 13698–13701.
Liu, Y., Ma, H., Zhang, Y., Pang, X., Fan, D., Wu, D., Wei, Q., 2016. Biosens. Bioelectron. 86, 439–445.
Lubin, A.A., Vander Stoep Hunt, B., White, R.J., Plaxco, K.W., 2009. Anal. Chem. 81, 2150–2158.
Ren, K., Wu, J., Yan, F., Ju, H., 2014. Sci. Rep. 4, 4360–4365.
Ren, K., Wu, J., Yan, F., Zhang, Y., Ju, H., 2015. Biosens. Bioelectron. 66, 345–349.
Rohs, R., Sklenar, H., 2004. J. Biomol. Struct. Dyn. 21, 699–711.
Rohs, R., Sklenar, H., Lavery, R., Röder, B., 2000. J. Am. Chem. Soc. 122, 2860–2866.
Rowe, A.A., Chuh, K.N., Lubin, A.A., Miller, E.A., Cook, B., Hollis, D., Plaxco, K.W., 2011. Anal. Chem. 83, 9462–9466.
Shen, J., Wang, H.Y., Li, C.X., Zhao, Y.Y., Yu, X.J., Luo, X.L., 2017. Biosens. Bioelectron. 90, 356–362.
Song, P., Xiang, Y., Xing, H., Zhou, Z., Tong, A., Lu, Y., 2012. Anal. Chem. 84, 2916–2922.
Steel, A.B., Herne, T.M., Tarlov, M.J., 1998. Anal. Chem. 70, 4670–4677.
Sun, C., Liu, X., Feng, K., Jiang, J., Shen, G., Yu, R., 2010. Anal. Chim. Acta 669, 87–93.
Sun, J., Jiang, W., Zhu, J., Li, W., Wang, L., 2015. Biosens. Bioelectron. 70, 15–20.
Tuite, E., Norden, B., 1994. J. Am. Chem. Soc. 116, 7548–7556.
Wang, L., Ma, R., Jiang, L., Jia, L., Jia, W., Wang, H., 2017. Biosens. Bioelectron. 92, 390–395.
Wang, T., Viennois, E., Merlin, D., Wang, G., 2015. Anal. Chem. 87, 8173–8180.
Wu, D., Yin, B.-C., Ye, B.-C., 2011. Biosens. Bioelectron. 28, 232–238.
Wu, L., Zhang, X., Liu, W., Xiong, E., Chen, J., 2013a. Anal. Chem. 85, 8397–8402.
Wu, Y., Lai, R.Y., 2013b. Chem. Commun. 49, 3422–3424.
Wu, Y., Lai, R.Y., 2016. Anal. Chem. 88, 2227–2233.
Xiao, Y., Lou, X., Uzawa, T., Plakos, K.J., Plaxco, K.W., Soh, H.T., 2009. J. Am. Chem. Soc. 131, 15311–15316.
Xiao, Y., Lubin, A.A., Baker, B.R., Plaxco, K.W., Heeger, A.J., 2006. Proc. Natl. Acad. Sci. USA 103, 16677–16680.
Xiao, Y., Lubin, A.A., Heeger, A.J., Plaxco, K.W., 2005a. Angew. Chem. Int. Ed. 117, 5592–5595.
Xiao, Y., Piorek, B.D., Plaxco, K.W., Heeger, A.J., 2005b. J. Am. Chem. Soc. 127, 17990–17991.
Xiao, Y., Qu, X., Plaxco, K.W., Heeger, A.J., 2007a. J. Am. Chem. Soc. 129, 11896–11897.
Xiao, Y., Rowe, A.A., Plaxco, K.W., 2007b. J. Am. Chem. Soc. 129, 262–263.
Xiong, E., Zhang, X., Liu, Y., Zhou, J., Yu, P., Li, X., Chen, J., 2015. Anal. Chem. 87, 7291–7296.
Yang, A.H., Hsieh, K., Patterson, A.S., Ferguson, B.S., Eisenstein, M., Plaxco, K.W., Soh, H.T., 2014. Angew. Chem. 126, 3227–3231.
Yang, K., Zhang, C.-Y., 2010. Anal. Chem. 82, 9500–9505.
Zhang, H.-R., Xu, J.-J., Chen, H.-Y., 2013. Anal. Chem. 85 (11), 5321–5325.
Zhang, J., Song, S., Zhang, L., Wang, L., Wu, H., Pan, D., Fan, C., 2006. J. Am. Chem. Soc. 128 (26), 8575–8580.
Zhang, L., Han, Y., Zhao, F., Shi, G., Tian, Y., 2015. Anal. Chem. 87, 2931–2936.
Zhang, S., Xia, J., Li, X., 2008. Anal. Chem. 80, 8382–8388.
Zhu, X., Zhang, Y.S., Yang, W.Q., Liu, Q.D., Lin, Z.Y., Qiu, B., Chen, G.N., 2011. Anal. Chim. Acta 684, 121–125.